

## Relativistic description of $\Lambda$ , $\Sigma$ , and $\Xi$ hypernuclei

J. Mareš\* and B. K. Jennings

TRIUMF, 4004 Wesbrook Mall, Vancouver, British Columbia, Canada V6T 2A3

(Received 30 November 1993; revised manuscript received 23 December 1993)

Characteristics of  $\Lambda$ ,  $\Sigma$ , and  $\Xi$  hypernuclei are investigated within the relativistic mean-field theory. The spin-orbit splitting is very sensitive to the value of tensor coupling  $f_{\omega Y}$ . A self-consistent treatment together with elimination of the hyperon self-coupling contribution is crucial for determining the  $V_\rho$  contribution to the hyperon binding.

PACS number(s): 21.10.-k, 21.60.-n, 21.80.+a

### I. INTRODUCTION

In this work, we study  $\Lambda$ ,  $\Sigma$ , and  $\Xi$  hypernuclei in the framework of the relativistic mean-field approximation. This approach is very successful in a description of ordinary nuclei [1,2].

Early works [3,4] for  $\Lambda$  hypernuclei achieved success (particularly in getting a weak spin-orbit force) by taking significantly weaker strengths for the meson couplings to the  $\Lambda$  than for the nucleons. More recently it has been suggested [5–9] that larger values of the meson couplings, consistent with SU(3), can be used if the tensor couplings are taken into account. This approach has been extended [8] beyond the  $\Lambda$  to other strange baryons using SU(3). Unfortunately, the works that studied the hypernuclear tensor couplings so far have restricted themselves to more or less qualitative estimates and used a shell model approach with *a priori* fixed potentials.

Recent calculations of  $\Lambda$  and  $\Sigma$  hypernuclei by Glendenning *et al.* [10] use only partially self-consistent potentials (determined for the nuclear core within the relativistic Thomas-Fermi approximation) and moreover omit the tensor couplings of vector mesons.

Our aim is to discuss the couplings of hyperons to different mesonic fields and their implications for  $\Lambda$ ,  $\Sigma$ , and  $\Xi$  hypernuclei. We demonstrate the different effects of the meson fields in particular hypernuclear systems and study the effects of the tensor coupling on the spin-orbit splittings. Complications that arise with the inclusion of the  $\rho$  meson are also discussed.

In contrast to Brockmann and Weise [3], Boguta and Bohrmann [4], and recent numerous studies of (multi)strange systems [11] we use couplings consistent with SU(3) [12]. This is the first fully self-consistent calculation of  $\Lambda$ ,  $\Sigma$ ,  $\Xi$  hypernuclei that includes the tensor couplings.

After a brief description of the model in Sec. II and

discussion of the hyperon-meson coupling constants in Sec. III, the results are presented in Sec. IV. The conclusions are drawn in Sec. V.

### II. MODEL

The model of relativistic quantum field theory [1], which forms the framework for our investigations, describes the nucleus as a system of Dirac spinors (nucleons) interacting via meson fields in the mean-field approximation. Here we study hypernuclear systems and thus extend the original model for ordinary nuclei to the strange particle ( $\Lambda$ ,  $\Sigma$ ,  $\Xi$ ) sector. We start from a Lagrangian density of the form

$$\mathcal{L} = \mathcal{L}_N + \mathcal{L}_Y, \quad Y = \Lambda, \Sigma, \Xi, \quad (1)$$

$$\begin{aligned} \mathcal{L}_Y = & \bar{\Psi}_Y [i \gamma_\mu \partial^\mu - g_{\omega Y} \gamma_\mu V^\mu - (M_Y + g_{\sigma Y} \phi)] \Psi_Y \\ & + \mathcal{L}_T + \mathcal{L}_{\rho Y} + \mathcal{L}_{AY}. \end{aligned} \quad (2)$$

Here,  $\mathcal{L}_N$  is the standard Lagrangian of mean-field theory [1,2]. It involves nucleons ( $\Psi_N$ ), scalar  $\sigma$  mesons ( $\phi$ ), vector  $\omega$  mesons ( $V^\mu$ ), vector isovector  $\rho$  mesons ( $\mathbf{b}^\mu$ ), and the photon ( $A^\mu$ ) (for the Coulomb field). The scalar meson self-couplings  $\mathcal{L}_{nl} = -\frac{1}{3}g_2 \phi^3 - \frac{1}{4}g_3 \phi^4$  are included, as well.

The Lagrangian density  $\mathcal{L}_Y$  that describes the hyperon  $\Psi_Y$  and its couplings to mesonic fields includes the  $\omega$ - $Y$  coupling term  $\mathcal{L}_T$ ,

$$\mathcal{L}_T = \frac{f_{\omega Y}}{2M_Y} \bar{\Psi}_Y \sigma^{\mu\nu} \partial_\nu V_\mu \Psi_Y. \quad (3)$$

The last two terms  $\mathcal{L}_{\rho Y}$  and  $\mathcal{L}_{AY}$  in Eq. (2) describe the interactions of a hyperon with the  $\rho$  meson and Coulomb field. For a particular hyperon they acquire the following form:

$$\mathcal{L}_{\rho\Lambda} + \mathcal{L}_{A\Lambda} = 0, \quad \text{since } \Lambda \text{ is neutral and isoscalar,} \quad (4)$$

$$\mathcal{L}_{\rho\Xi} + \mathcal{L}_{A\Xi} = -\bar{\Psi}_\Xi \left[ \frac{1}{2} g_{\rho\Xi} \gamma_\mu \mathbf{b}^\mu \cdot \boldsymbol{\tau}_\Xi + \frac{e}{2} (\tau_{3,\Xi} - 1) \gamma_\mu A^\mu \right] \Psi_\Xi, \quad (5)$$

\*Permanent address: Nuclear Physics Institute, 25068 Řež, Czech Republic.

$$\mathcal{L}_{\rho\Sigma} + \mathcal{L}_{A\Sigma} = -\bar{\Sigma}_{ij} \left( \frac{g_{\rho\Sigma}}{2} \gamma_{\mu} \Theta_{jk}^{\mu} + \frac{e}{2} \gamma_{\mu} A^{\mu} (\tau_{3,\Sigma})_{jk} \right) \Sigma_{ki} \quad [10], \quad (6)$$

where

$$\Sigma_{ij} = \begin{pmatrix} \Psi_{\Sigma^0} & \sqrt{2}\Psi_{\Sigma^+} \\ \sqrt{2}\Psi_{\Sigma^-} & -\Psi_{\Sigma^0} \end{pmatrix} \quad (7)$$

and

$$\Theta_{ij}^{\mu} = \begin{pmatrix} \rho_0^{\mu} & \sqrt{2}\rho_+^{\mu} \\ \sqrt{2}\rho_-^{\mu} & -\rho_0^{\mu} \end{pmatrix} . \quad (8)$$

The Lagrangian (1) is treated in the mean-field and the no-sea approximations [2]; the contributions of anti(quasi)particles and quantum fluctuations of meson fields are thus neglected. The equations of motion derived from the Lagrangian (1) by standard techniques are the Dirac equations for baryons and the inhomogeneous Klein-Gordon equations for the meson fields. In the static limit they read

$$\left[ -i\boldsymbol{\alpha} \cdot \boldsymbol{\nabla} + g_{\omega i} V_0 + \beta (M_i + g_{\sigma i} \phi) - \delta_{Yi} i \frac{f_{\omega Y}}{2M_Y} \beta \boldsymbol{\alpha} \cdot \boldsymbol{\nabla} V_0 + I_{3i} g_{\rho i} b_0 + Q_i e A_0 \right] \psi_{\alpha i} = \epsilon_{\alpha i} \psi_{\alpha i} , \quad (9)$$

$i = N, \Lambda, \Sigma, \Xi ,$

$$(-\Delta + m_j^2) B_j = \sum_i g_{ji} \rho_{ji} - \delta_{iY} \delta_{j\omega} \frac{f_{\omega}}{2M_Y} \rho_T + \delta_{j\sigma} (-g_2 \phi^2 - g_3 \phi^3) , \quad (10)$$

$$-\Delta A_0 = e \sum_i \rho_{ci} . \quad (11)$$

Here,

$$\rho_{ji} = \sum_{\alpha}^{\text{occ}} \bar{\psi}_{\alpha i} D_j \psi_{\alpha i} , \quad j = \sigma, \omega_0, \rho_0 ,$$

$$\rho_{ci} = \sum_{\alpha}^{\text{occ}} \bar{\psi}_{\alpha i} Q_i \psi_{\alpha i} ,$$

$$\rho_T = \boldsymbol{\nabla} \sum_{\alpha}^{\text{occ}} \bar{\psi}_{\alpha i} i\boldsymbol{\alpha} \psi_{\alpha i} ,$$

$$D_{\sigma} = -1, \quad D_{\omega_0} = \gamma_0, \quad D_{\rho_0} = \gamma_0 I_{3i} ,$$

$$B_{\sigma} = \phi, \quad B_{\omega_0} = V_0, \quad B_{\rho_0} = b_0 ,$$

and  $\alpha$  in summations runs over all occupied particle states.  $I_{3i}$  and  $Q_i$  are the third isospin component and the charge of the baryon, respectively:

$$I_{3i} = \frac{1}{2} \tau_3 \quad \text{for } i = N, \Xi ,$$

$$1, 0, -1 \quad \text{for } i = \Sigma^+, \Sigma^0(\Lambda), \Sigma^-, \text{ respectively,}$$

$$Q_i = \frac{1}{2} (1 + \tau_3) \text{ for } N,$$

$$\frac{1}{2} (\tau_3 - 1) \text{ for } \Xi ,$$

$$I_3 \quad \text{for } \Sigma (\Lambda) .$$

The coupled system of field equations (9–11) for both baryons ( $N, Y$ ) and meson fields  $\phi, V_0, b_0, A_0$  was solved self-consistently using iterative procedure of Ref. [13]. The self-consistency was important particularly for evaluation of the contribution of the isovector  $\rho$  field to the

predictions of hyperon binding energies as will be seen in Sec. IV. The methods of solution used in Refs. [9,10] omitted the contribution of the hyperon to the source terms of meson field equations (10 and 11) and thus the modification of the mean fields due to the additional hyperon. This consequently led to different conclusions.

Finally, the following is to be noted.

(i) The spatial components of vector fields  $\mathbf{V}, \mathbf{b}, \mathbf{A}$  were not included in our calculations since they were not subject to the study in this work and, moreover, they are of little importance in spectroscopic calculations of nuclear systems, as was pointed out in Refs. [14,15]. On the other hand, retaining the spatial components  $\mathbf{V}$  in the Hartree calculations of the entire “core+1” system is crucial for a consistent inclusion of the effect of the nuclear core response. (The effect of a hyperon on the nuclear core was studied in detail by Cohen and Furnstahl [16], extended later by Cohen and Noble [17], and Cohen [15].)

(ii) The tensor coupling terms for nucleons were omitted due to a negligible  $f_{\omega N}$  coupling constant.

(iii) The effect of the anomalous coupling  $f_{\rho Y}$  was tested in several cases and since it was found to be very small the  $\rho$ - $Y$  tensor coupling terms were neglected.

### III. PARAMETRIZATION

For the nucleonic sector we used the parameter set of Sharma *et al.* [18] that describes properties of nuclear matter as well as of finite nuclei reasonably well.

TABLE I. The parametrization of the nucleonic sector (adopted from Ref. [18]). The masses are given in MeV and the coupling  $g_2$  in  $\text{fm}^{-1}$ .

$M_N$	939.0	$g_{\sigma N}$	10.444
$m_\sigma$	526.065	$g_{\omega N}$	12.945
$m_\omega$	783.0	$g_{\rho N}$	8.766
$m_\rho$	763.0	$g_2$	-6.9099
		$g_3$	-15.8337

Moreover, this model is numerically more stable than the widely used model NL1 [19] for which the barrier to the instability is already below the central density in  $^{12}\text{C}$  [2]. The masses and coupling constants of the model used are listed in Table I.

For the coupling of the  $\omega$  meson to the hyperons we have used the naive quark model values of the ratio to the  $\omega$ -nucleon coupling. There is a nice discussion of these values in a paper by Dover and Gal [12] and we have taken our results directly from there [see their Eqs. (2.8) and (2.23)]. The  $\rho$  couplings are not given; however, they can be easily determined by the same techniques using the SU(3) Clebsch-Gordan coefficients (see, for example, Ref. [20] for the coefficients).

For illustration of the effect of the  $\omega YY$  tensor coupling to the value of the spin-orbit splitting in hypernuclei, we adopted for  $f_{\omega Y}$  also values from Nijmegen models  $F$  [21] and  $D$  [22] and values suggested by Cohen and Weber [8].

The values of  $\alpha_{\sigma Y} = g_{\sigma Y}/g_{\sigma N}$ ,  $\alpha_{\omega Y} = g_{\omega Y}/g_{\omega N}$ ,  $\alpha_{\rho Y} = g_{\rho Y}/g_{\rho N}$ , and  $\alpha_{TY} = f_{\omega Y}/g_{\omega Y}$  for all the models used are presented in Table II.

While the values of  $g_{\omega Y}$  coupling constants were determined from the naive quark model, namely;

$$g_{\omega\Lambda} = g_{\omega\Sigma} = 2g_{\omega\Xi} = \frac{2}{3}g_{\omega N}, \quad (12)$$

the values of  $g_{\sigma Y}$  were deduced from the available experimental information on hyperon binding in the nuclear medium. This gave a coupling close to the expected value of two-thirds that for the nucleon. However, the hypernuclear levels are very sensitive to the coupling's precise value due to large cancellations and therefore this coupling was adjusted to get quantitative agreement with the hypernuclear levels.

For the  $\Lambda$  hyperon  $g_{\sigma\Lambda}$  was fitted so as to reproduce the binding energy of a  $\Lambda$  in the  $s$  state of  $^{17}_\Lambda\text{O}$ . The parametrization with  $g_{\sigma\Lambda}$  determined from only this one experimental value already gives a reasonable description of binding energies of  $\Lambda$  in hypernuclei for a wide range of mass numbers,  $A=5-89$  [23]. For the sake of illustration we present Fig. 1 with the  $\Lambda$  binding energies for several

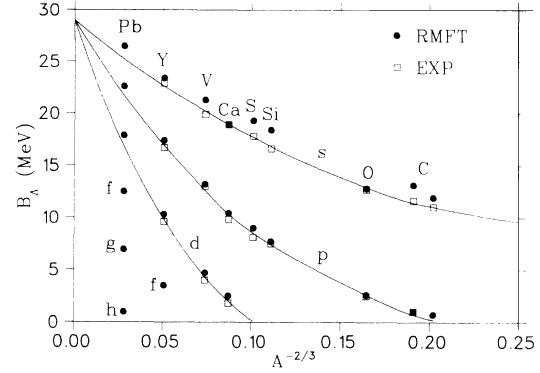


FIG. 1. Comparison of the  $\Lambda$  single-particle energies for parametrizations from Table I and  $f_{\omega\Lambda}/g_{\omega\Lambda} = -1$  with experimental data [28].

hypernuclei between  $^{12}_\Lambda\text{C}$  and  $^{209}_\Lambda\text{Pb}$ . Smaller values of  $\alpha_{i\Lambda}$ , namely,  $\alpha_{i\Lambda} \approx 0.3-0.4$  ( $i = \sigma, \omega$ ), would give better agreement with the data [23].

Due to insufficient experimental information on  $\Sigma$  and  $\Xi$  hypernuclei, we chose  $g_{\sigma i}$  ( $i = \Sigma, \Xi$ ) to roughly obtain the estimated  $\Sigma(\Xi)$  potential depth in nuclear matter. Interpretation of scarce events of  $\Xi^-$  hypernuclei observed in emulsion experiments with  $K^-$  beams [24] leads to a potential well depth  $U_\Xi \approx 20-25$  MeV. A similar value for a  $\Sigma$  embedded in nuclear matter ( $U_\Sigma \approx 20-30$  MeV) was deduced from the level shifts in  $\Sigma^-$  atoms [25].

The values of  $g_{\sigma Y}$  ( $Y = \Sigma, \Xi$ ) presented in Table II give  $U_Y \approx 25-30$  MeV. (In fact, the value of  $g_{\sigma\Xi}$  was adopted from Ref. [26].) The smaller  $g_{\sigma\Sigma}$  compared to  $g_{\sigma\Lambda}$  compensates the mass difference  $M_\Sigma - M_\Lambda$  that would lead to a stronger binding of  $\Sigma^0$  in the same potential well.

We have neglected the finite width of the  $\Sigma$  hyperon states due to  $\Sigma N \rightarrow \Lambda N$  conversion and  $\Sigma N \rightarrow \Sigma N$  charge exchange. It can be incorporated schematically by introducing an absorptive potential for  $\Sigma$  hyperons [25,10]. However, the question of the width of the  $\Sigma$  hypernuclear states is an open problem that is beyond the scope of this work.

#### IV. RESULTS

We calculated several  $\Lambda$ ,  $\Sigma$ ,  $\Xi$  hypernuclei using the sets of coupling constants and masses listed in Tables I and II. Several values of the tensor coupling for each hypernucleus were used in order to investigate the sensitivity of the position of single-particle levels to the strength

TABLE II. The couplings used for the hyperonic sector. The ratios of hyperon to nucleon couplings for  $Y = \Lambda, \Sigma$ , and  $\Xi$  are presented here. For  $\alpha_{TY}$  the values of Nijmegen models  $F$  [21],  $D$  [22], and the values adopted from Cohen and Weber [8] and from Dover and Gal [12] are used for comparison.

	$\alpha_{\sigma Y} = g_{\sigma Y}/g_{\sigma N}$	$\alpha_{\omega Y} = g_{\omega Y}/g_{\omega N}$	$\alpha_{\rho Y} = g_{\rho Y}/g_{\rho N}$	$\alpha_{TY} = f_{\omega Y}/g_{\omega Y}$				
$\Lambda$	0.621	0.667	0.0	0.0	-0.122 [22]	-0.541 [21]	-1.0	—
$\Sigma$	0.619	0.667	1.0	0.0	0.76 [12]	—	1.0	1.417 [22]
$\Xi$	0.375	0.333	1.0	0.0	-0.4 [22]	-1.89 [8, 21]	-2.0	-2.27 [8]

of  $f_{\omega Y}$ .

In Figs. 2(a-c) and 3(a-c) we present results of calculations for  $^{17}_Y\text{O}$  and  $^{41}_Y\text{Ca}$ , respectively. For illustration and better comparison of the role of the tensor coupling for different hyperons we have chosen systems with neutral particles and omitted the  $\rho$  meson coupling for  $\Xi$ .

The figures illustrate the quite different evolution of the spin-orbit (s.o.) splitting for the three kinds of hyperons. The  $\Lambda$  hypernuclear splitting from Figs. 2(a) and 3(a) is gradually decreasing with increasing  $\alpha_{T\Lambda}$  from 1.56 MeV for  $\alpha_{T\Lambda} = 0$  to 0.23 MeV for  $\alpha_{T\Lambda} = -1.0$ . On the other hand, the s.o. splitting in  $\Sigma$  hypernuclei [Figs. 2(b) and 3(b)] increases due to a positive  $f_{\omega\Sigma}$  (see the following expression for s.o. force  $V_{ls}^Y$ ). For the quark model  $\alpha_{T\Sigma} = 1.0$  it acquires almost double the value for  $\alpha_{T\Sigma} = 0$ . Extremely large negative values of  $f_{\omega\Xi}$  for the  $\Xi$  hyperon result even in a change of the level ordering as can be seen in Figs. 2(c) and 3(c).

It is worthy to mention the observed shift of the  $s_{1/2}$  state after inclusion of the tensor coupling. The positive (negative) value of  $f_{\omega Y}$  leads to a decrease (increase) of the  $s_{1/2}$  single-particle energy of a hyperon as can be seen in Figs. 2 and 3.

Summarizing the results of Figs. 2 and 3 we obtain the following relation between hypernuclear spin-orbit splittings:

$$V_{s.o.}^{\Lambda} \approx 1.1V_{s.o.}^{\Sigma} \approx 2.7V_{s.o.}^{\Xi} \approx 0.3V_{s.o.}^N \quad \text{for } \alpha_{TY} = 0 ,$$

$$V_{s.o.}^{\Lambda} \approx 0.09V_{s.o.}^{\Sigma} \approx -0.5V_{s.o.}^{\Xi} \approx 0.04V_{s.o.}^N$$

for quark model values of  $\alpha_{TY}$ .

Figures 2 and 3 confirm that the inclusion of the  $\omega Y$  tensor coupling causes large changes in the hypernuclear spin-orbit splitting as predicted in Refs. [7-9,6]. Our calculations are in agreement with the numerical estimates of Cohen and Weber [8]. They predicted for the  $\Lambda$  hyperon spin-orbit interaction the reduction by a factor of about 10 relative to the pure  $\sigma$ - $\omega$  model, for the  $\Sigma$  hyperon increase by about 50% - 100% (depending on  $\alpha_{T\omega}$  used), and the  $\Xi$  hyperon spin-orbit interaction about -15% to -20% of that of the nucleon.

The above results can be understood by recasting the Dirac equation in Schrödinger equivalent form [27] with the spin-orbit term

$$V_{ls}^Y \mathbf{l} \cdot \mathbf{s} = \frac{1}{2M_{\text{eff}}^2} \left[ \frac{1}{r} \left( g_{\omega\Lambda} V_0' - g_{\sigma\Lambda} \phi' + 2f_{\omega\Lambda} \frac{M_{\text{eff}}}{M_{\Lambda}} V_0' \right) \right] \mathbf{l} \cdot \mathbf{s} ,$$

$$M_{\text{eff}} = M_{\Lambda} - \frac{1}{2} (g_{\omega\Lambda} V_0 - g_{\sigma\Lambda} \phi) .$$

For  $f_{\omega Y} = 0$  the spin-orbit splitting ( $V_{s.o.}^Y$ ) for hyperons is reduced when compared to that for nucleons due to a larger mass  $M_{\text{eff}}$  in the denominator and due to the smaller couplings to  $\sigma$  and  $\omega$  mesons. The tensor couplings of the  $\omega$  to  $\Lambda$ ,  $\Sigma$ ,  $\Xi$  hyperons predicted by the quark model differ in their magnitudes and signs and hence their contribution to the spin-orbit term is thus different. This contribution is comparable in magnitude with the original  $\sigma$ - $\omega$  part and is negative (positive) for  $\Lambda$  ( $\Sigma$ ). It is negative and even larger than the  $\sigma$ - $\omega$  term

for  $\Xi$ . This results in (i) an almost cancellation of the s.o. term for  $\Lambda$ , (ii) an almost double enhancement of the s.o. term for  $\Sigma$ , and (iii) a change of the sign of the s.o. term for  $\Xi$ .

We should, however, bear in mind that although the effects of tensor coupling are relatively large, the absolute shifts in energy levels amount to less than 1 MeV and this is still beyond the reach of contemporary experimental resolution [28]. Figure 4 illustrates the size of the changes of the binding energy of  $\Sigma^0$  ( $B_{\Sigma^0}$ ) in O, Ca, Zr, Pb caused

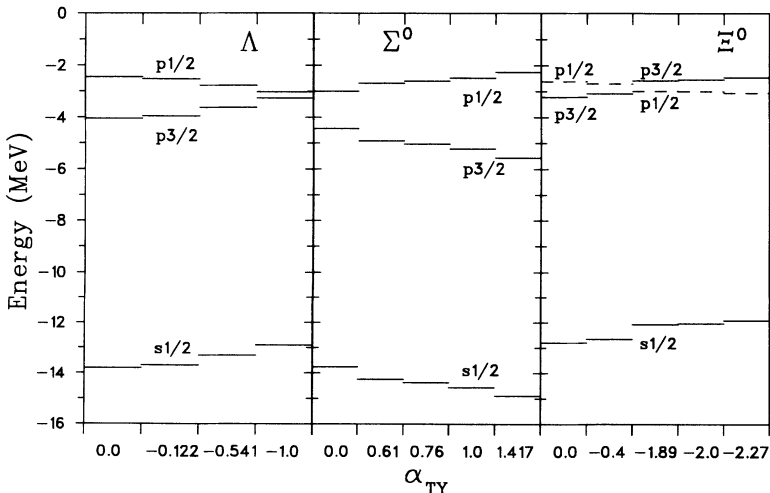


FIG. 2. Dependence of the position of the hyperon single-particle levels in  $^{17}_Y\text{O}$  ( $Y = \Lambda, \Sigma^0, \Xi^0$ ) on the  $\alpha_{TY} = f_{\omega Y}/g_{\omega Y}$  from Table II (a) for  $Y = \Lambda$ , (b) for  $Y = \Sigma^0$ , and (c) for  $Y = \Xi^0$ .

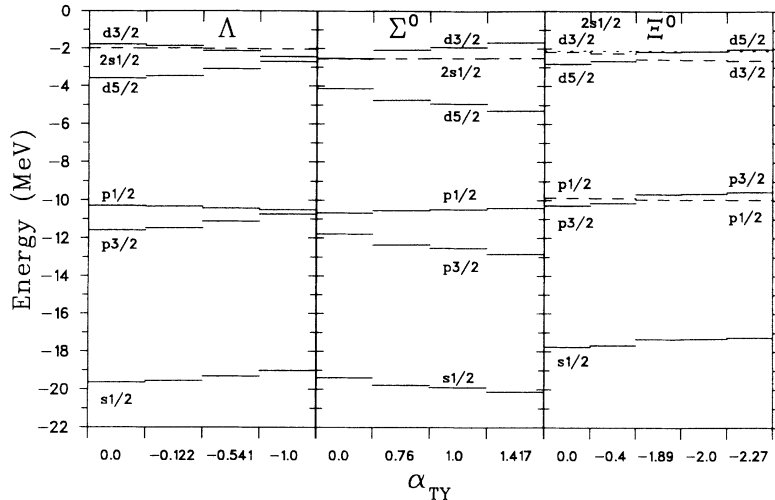


FIG. 3. Dependence of the position of the hyperon single-particle levels in  $^{41}\text{Ca}$  ( $Y = \Lambda, \Sigma^0, \Xi^0$ ) on the  $\alpha_{TY} = f_{\omega Y}/g_{\omega Y}$  (a) for  $Y = \Lambda$ , (b) for  $Y = \Sigma^0$ , and (c) for  $Y = \Xi^0$ .

by an inclusion of the tensor coupling term with  $\alpha_{T\Sigma} = 1$  (for  $p, d$  and higher orbits averaged values of  $B_{\Sigma^0}$  are presented).

The evolution of the binding energies of a neutral  $\Sigma^0$  in Fig. 4 is similar to that of  $\Lambda$  hypernuclei as can be seen from comparison with Fig. 1. The apparently slower increase in binding with  $A$  for  $\Sigma^0$  can be attributed to the  $\Sigma - \Lambda$  mass difference. The same holds for  $\Xi^0$  (for  $\alpha_{T\Sigma} = 0$ ) [from Fig. 6(b)].

Figures 4, 5, for  $\Sigma^0, \Sigma^-, \Sigma^+$  hypernuclei and Fig. 6 for  $\Xi^-, \Xi^0$  demonstrate the importance of the Coulomb interaction and  $g_{\rho Y}$  coupling for the systems under consideration.

At first, let us discuss the results of calculations when the  $\rho Y$  coupling is omitted ( $\alpha_{\rho Y} = 0$ ). The attractive Coulomb interaction for  $\Sigma^-$  [Fig. 5(a)] leads to a considerable stronger binding of  $\Sigma^-$  in the nuclear medium when compared with  $\Sigma^0$  hypernuclei from Fig. 4. This allows the population of highly excited hypernuclear states as was predicted by Glendenning *et al.* [10]. Similar results were obtained for  $\Xi^0$  and  $\Xi^-$  hypernuclei [Figs. 6(a,b)].

For  $\Sigma^+$  the repulsive Coulomb potential decreases the binding of  $\Sigma^+$  [see Fig. 5(b)]. Consequently only  $s$  and  $p$  bound states were found in  $\Sigma^+$  hypernuclei for  $\alpha_{\rho\Sigma} = 0$ . The effect of Coulomb repulsion increases in heavier

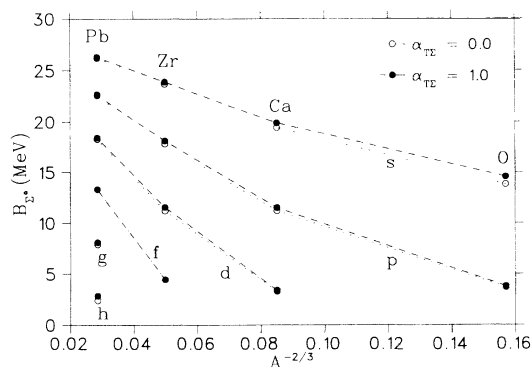


FIG. 4.  $\Sigma^0$  single-particle levels in O, Ca, Zr, Pb for  $\alpha_{T\Sigma} = 0$  and  $\alpha_{T\Sigma} = 1$ .

hypernuclei with large charge number ( $Z$ ) leading even to decreasing binding  $B_{\Sigma^+}$  when going from Ca to Pb.

The  $\rho$  meson coupling to hyperons affects the previous results appreciably. When directly solving Eqs. (9)–(11) with  $\rho$ -hyperon couplings from Table II, there are extremely large shifts in the positions of the hyperon single-particle levels even in hypernuclei with an isospin saturated core (O, Ca). For example, after including the  $\rho$ -hyperon interaction the  $s1/2$  single-particle energy of

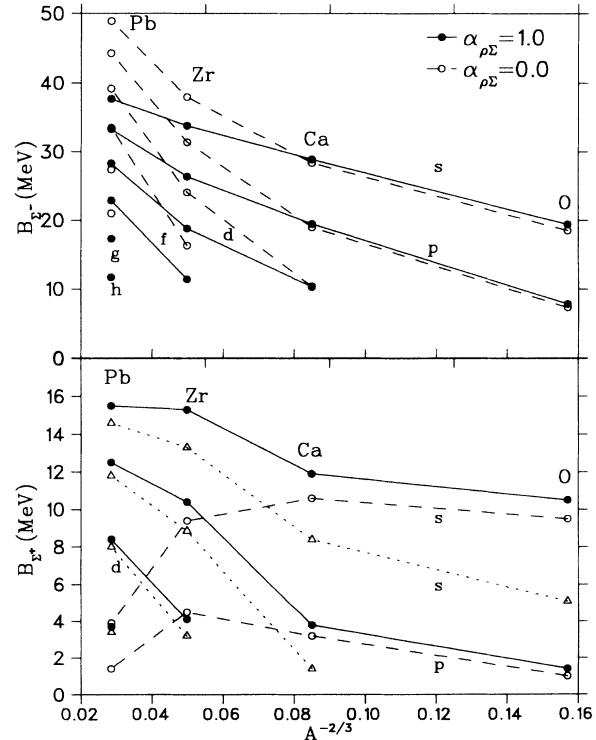


FIG. 5. Comparison of the  $\Sigma^-$  [upper part (a)] and the  $\Sigma^+$  [lower part (b)] single-particle levels in O, Ca, Zr, Pb for  $\alpha_{\rho\Sigma} = 0$  and  $\alpha_{\rho\Sigma} = 1$ ;  $\alpha_{T\Sigma} = 1$ . Dotted lines in (b) illustrate the effect of the  $\rho$  meson field with the spurious hyperon self-coupling contribution (see text).

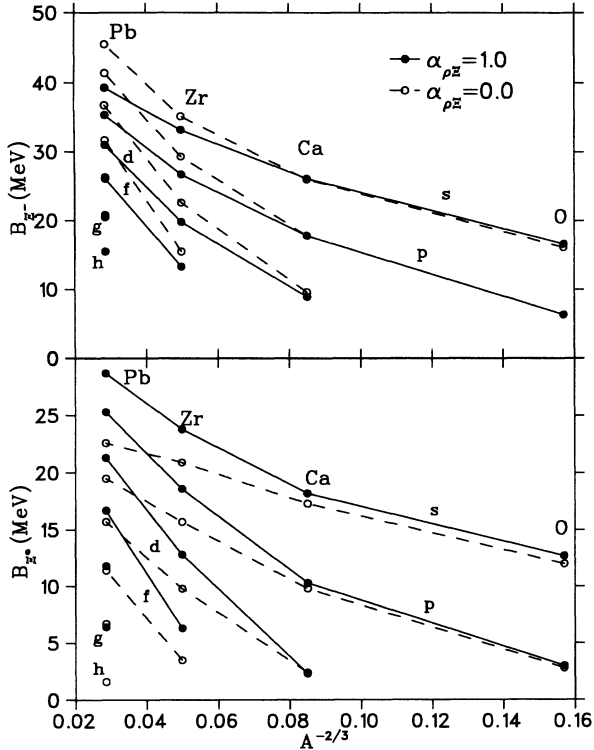


FIG. 6. Comparison of the  $\Xi^-$  [upper part (a)] and the  $\Xi^0$  [lower part (b)] single-particle levels in O, Ca, Zr, Pb for  $\alpha_{\rho\Xi} = 0$  and  $\alpha_{\rho\Xi} = 1$ ;  $\alpha_{T\Sigma} = 1$ .

$\Sigma^+$  in  $^{17}_{\Sigma^+}\text{O}$  decreased by 4.4 MeV [compare dashed and dotted curves in Fig. 5(b)].

However, it was pointed out by Gal [29] that the main contribution to this  $\rho$ -coupling effect is spurious. For a pure isospin-zero core the entire  $\rho$  field is generated by the hyperon. The Hartree approximation includes this field in the potential for the hyperon. Thus in this case the entire effect of the  $\rho$  is due to the hyperon interacting with itself, i.e., the hyperon self-energy due to the  $\rho$ . For real hypernuclei the core, even with an  $N = Z$ , will not be pure isospin zero due to Coulomb effects and the polarization from the hyperon. Consequently a nonzero real  $\rho$  contribution will remain. The “spurious” contribution would be largely eliminated by a careful treatment of the mass renormalization of the hyperon. The Hartree-Fock approximation automatically treats the self-energy terms correctly [30]. Brockmann [30] found out that excluding these terms for  $\sigma$  and  $\omega$  potentials in the Hartree approach affects the single-particle energies less than about 15%. For the  $V_\rho$  potential a considerably larger effect can be expected.

We have isolated the “spurious”  $Y$ - $\rho$  ( $Y = \Sigma, \Xi$ ) self-interaction terms by switching off the  $\rho$  coupling to the nucleons while the  $Y$ - $\rho$  interaction was left unchanged. By comparing the results with those for  $g_{\rho N} = g_{\rho Y} = 0$ , we obtained this spurious contribution of the hyperon self-interaction, which we then subtracted from the results of the full calculations. The solid lines in Figs. 5 and 6 represent already the results after subtracting these

“spurious” contributions.

The resulting  $\rho$  contribution is repulsive for both  $\Sigma^-$  and  $\Xi^-$  in Zr and Pb and thus compensates to some extent the effect of the attractive Coulomb potential. In Pb [Figs. 5(a) and 6(a)] the  $s_{1/2}$  level is shifted by 11 MeV and 6 MeV for  $\Sigma^-$  and  $\Xi^-$ , respectively. For hypernuclei with an  $N = Z$  core (O, Ca) the  $\rho$  contribution to  $\Sigma^-$  and  $\Xi^-$  binding is slightly attractive leading to shifts up to 1 MeV in hyperon single-particle energies.

The  $V_\rho$  potential is always attractive for all the  $\Sigma^+$ ,  $\Xi^0$  hypernuclei, again compensating the contribution of the Coulomb interaction. As before, the nonzero energy shifts (up to 1.4 MeV for the  $s$  state of  $\Sigma^+$  in Ca) are already encountered in systems with an  $N = Z$  core. The effect of the  $\rho$  field is more pronounced in  $\Sigma^+$  hypernuclei due to a relatively stronger  $\rho$ - $\Sigma$  coupling [compare Figs. 5(b) and 6(b)]. As a result, the binding  $B_{\Sigma^+}$  converts from a decreasing to an increasing function of  $A$  in the systems with a neutron excess [see values for Zr and Pb in Fig. 5(b)].

It is clear that this result strongly depends on the value of the  $g_{\rho Y}$  coupling constant. In Ref. [10] where  $\alpha_{\rho\Sigma} = 0.6$  was used, no such conversion of the slope was observed.

In Fig. 7 we compare the  $\rho$  meson  $V_\rho$ , Coulomb  $V_c$ , and the sum of the  $\sigma$  and  $\omega$  meson ( $V_{\sigma+\omega}$ ) contributions to the central potential  $V_Y$  for  $\Sigma^+$  in  $^{17}_{\Sigma^+}\text{O}$ ,  $V_Y = V_\rho + V_c + V_{\sigma+\omega}$ . For illustration we also present the potential ( $V_\rho^S$ ) with the spurious  $\Sigma$  self-interaction contribution as it comes out from the direct solution of Eqs. (9)–(11). The difference ( $V_\rho^S - V_\rho$ ) corresponds to the self-interaction term. Eliminating the spurious contribution leads just to the large shift from  $V_\rho^S$  to  $V_\rho$  and consequently to quite different predictions of the  $\Sigma$  binding in  $^{17}_{\Sigma^+}\text{O}$ , as can be seen from Fig. 5(b). Figure 7 demonstrates that although the magnitude of the  $V_\rho$  potential is much smaller than of the “full”  $V_\rho^S$ , it is still not negligible and so are the effects of  $\rho$  meson in the hypernuclei with an isospin saturated nuclear core. This result is a consequence of the approach used here and thus could not be observed by Glendenning *et al.* in Ref. [10] where the Dirac equations for hyperons were solved only once for meson fields determined from the nuclear core.

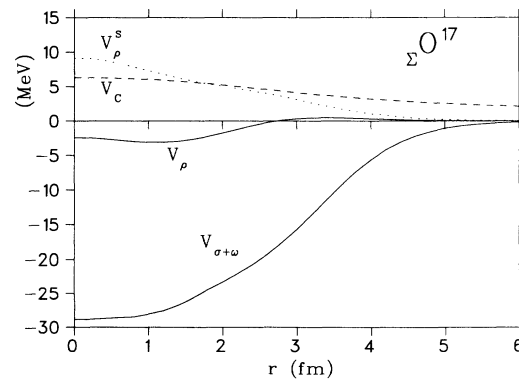


FIG. 7. Comparison of the different contributions to the central potential  $V_{\Sigma^+} = V_\rho + V_c + V_{\sigma+\omega}$  in  $^{17}_{\Sigma^+}\text{O}$ . The potential  $V_\rho^S$  that includes the hyperon self-coupling contribution is presented, as well.

## V. CONCLUSIONS

We performed self-consistent calculations of  $\Lambda$ ,  $\Sigma$ ,  $\Xi$  hypernuclei within the relativistic mean-field model that includes the  $\omega$ - $Y$  tensor coupling as well as  $\rho$  and  $A$  couplings to hyperons.

We have found larger effects of the tensor coupling of hyperons to the spin-orbit splitting than was predicted in Ref. [9,6]. (Note that in Ref. [9] there is an error and  $f = -g/2$  was actually used rather than the stated  $f = -g$ .) Our results are in agreement with the suggestions of Ref. [8]. When using quark model values for  $f_{\omega Y}$ , we obtain *7 times reduced* hypernuclear spin-orbit splitting in  ${}^{17}_{\Lambda}\text{O}$ , almost *twice as large* splitting for  $\Sigma$ , and even *changed level ordering* in  ${}^{17}_{\Xi}\text{O}$ . Unfortunately, even for  $\Lambda$  hypernuclei the effects encountered here are within the experimental resolution. It will thus be a task of future high resolution experiments to provide us with data from which the information on  $f_{\omega Y}$  coupling could be deduced.

We have witnessed large effects from the  $\rho$ -hyperon interaction in  $\Sigma$  and  $\Xi$  hypernuclei. Our treatment revealed nonzero shifts in the hyperon single-particle ener-

gies due to the  $V_{\rho}$  potential already in systems with an isospin saturated core (even after eliminating the spurious hyperon self-coupling). The results for  $\Xi$  hypernuclei suggest that it would be not only interesting but also desirable to extrapolate the considerations to multistrange baryonic systems, where we may expect that the inclusion of the strong  $g_{\rho\Xi}$  coupling will significantly modify the results obtained by Schaffner *et al.* [26] for  $g_{\rho\Xi} = 0$ . Calculations along these lines are in progress and will be published elsewhere [31].

Although the results for  $\Sigma$  and  $\Xi$  hypernuclei should be regarded as a qualitative estimate, they exhibit some general features that should remain valid after we learn more about  $YN$  interaction.

## ACKNOWLEDGMENTS

We are grateful to Avraham Gal for useful comments, discussions, and for a careful reading of the manuscript. One of the authors (B.K.J.) thanks the Natural Sciences and Engineering Research Council of Canada for financial support.

- 
- [1] B. D. Serot and J. D. Walecka, *Adv. Nucl. Phys.* **16**, 1 (1986).
  - [2] P.-G. Reinhard, *Rep. Prog. Phys.* **52**, 439 (1989).
  - [3] R. Brockmann and W. Weise, *Phys. Lett.* **69B**, 167 (1977).
  - [4] J. Boguta and S. Bohrmann, *Phys. Lett.* **102B**, 93 (1981).
  - [5] J.V. Noble, *Phys. Lett.* **89B**, 325 (1980).
  - [6] A. Bouyssy, *Nucl. Phys.* **A381**, 445 (1982).
  - [7] B. K. Jennings, *Phys. Lett. B* **246**, 325 (1990).
  - [8] J. Cohen and H. J. Weber, *Phys. Rev. C* **44**, 1181 (1991).
  - [9] M. Chiapparini, A. O. Gattone, and B. K. Jennings, *Nucl. Phys.* **A529**, 589 (1991).
  - [10] N. K. Glendenning, D. Von-Eiff, M. Haft, H. Lenske, and M. K. Weigel, *Phys. Rev. C* **48**, 889 (1993).
  - [11] M. Rufa, J. Schaffner, J. Maruhn, H. Stöcker, W. Greiner, and P.-G. Reinhard, *Phys. Rev. C* **42**, 2469 (1990); M. Rufa, H. Stöcker, J. Maruhn, P.-G. Reinhard, and W. Greiner, *J. Phys. G* **13**, 143 (1987); J. Mareš and J. Žofka, *Z. Phys. A* **333**, 209 (1989); **345**, 47 (1993).
  - [12] C. B. Dover and A. Gal, in *Progress in Particle and Nuclear Physics*, edited by D. Wilkinson (Pergamon Press, Oxford, 1984), Vol. 12, p. 171.
  - [13] C. J. Horowitz and B. D. Serot, *Nucl. Phys.* **A368**, 503 (1981).
  - [14] R. J. Furnstahl and B. D. Serot, *Nucl. Phys.* **A468**, 539 (1987).
  - [15] J. Cohen, *Phys. Rev. C* **48**, 1346 (1993).
  - [16] J. Cohen and R. J. Furnstahl, *Phys. Rev. C* **35**, 2231 (1987).
  - [17] J. Cohen and J. V. Noble, *Phys. Rev. C* **46**, 801 (1992).
  - [18] M. M. Sharma, M. A. Nagarajan, and P. Ring, *Phys. Lett.* **B312**, 377 (1993).
  - [19] P.-G. Reinhard *et al.*, *Z. Phys. A* **323**, 13 (1986).
  - [20] Particle Data Group, *Phys. Rev. D* **45**, S1 (1992).
  - [21] M. M. Nagels, T. A. Rijken, and J. J. de Swart, *Phys. Rev. D* **20**, 1633 (1979).
  - [22] M. M. Nagels, T. A. Rijken, and J. J. de Swart, *Phys. Rev. D* **12**, 744 (1975); **15**, 2547 (1977).
  - [23] J. Mareš, Report No. TRI-PP-93-102, 1993.
  - [24] C. B. Dover and A. Gal, *Ann. Phys. (N.Y.)* **146**, 309 (1983).
  - [25] C. B. Dover, D. J. Millener, and A. Gal, *Phys. Rep.* **184**, 1 (1989).
  - [26] J. Schaffner, C. B. Dover, A. Gal, C. Greiner, D. J. Millener, and H. Stöcker, *Ann. Phys. (N.Y.)* (to be published).
  - [27] J. D. Bjorken and S. D. Drell, *Relativistic Quantum Mechanics* (McGraw-Hill, New York, 1964).
  - [28] R. E. Chrien, *Nucl. Phys.* **A478**, 705c (1988).
  - [29] A. Gal (private communication).
  - [30] R. Brockmann, *Phys. Rev. C* **18**, 1510 (1978).
  - [31] J. Mareš (unpublished).